Headgroup Orientations of Alkyl Glycosides at a Lipid Bilayer Interface

Charles R. Sanders, II,† and James H. Prestegard*

Contribution from the Department of Chemistry, Yale University, New Haven, Connecticut 06511.
Received January 16, 1992

Abstract: A series of functionally related alkyl monoglycosides was prepared, and their headgroup orientations were examined using dipolar coupling data from ^{13}C NMR spectra in oriented liquid crystalline phases. The following ^{13}C-labeled compounds were synthesized: β-dodecyl galactopyranoside, β-tetradecyl 2-deoxyglucopyranoside, β-dodecyl 6-deoxyglucopyranoside, α-dodecyl glucopyranoside, α-tetradecyl 2-deoxyglucopyranoside, α-dodecyl 2,3-dideoxyglucopyranoside, and α-dodecyl 2,3-dideoxy-*erythro*-hex-2-enopyranoside. These glycolipid analogs were solubilized in oriented bilayers composed of 1,2-dimyristoyl-*sn*-3-glycerophosphocholine (DMPC) and 3-[(3-cholamidopropyl)dimethylammonio]-2-hydroxy-1-propanesulfonate (CHAPSO). The α-2,3-dideoxyglycosides induced an oriented to isotropic transition in the bilayers which precluded the measurement of dipolar coupling constants and further structural characterization. However, each of the other molecules examined yielded at least five $^{13}C-^{13}C/^{1}H-^{13}C$ coupling constants. In some cases, the anisotropy of the chemical shifts was also measured. The dipolar data sets were analyzed in structural terms using a general order matrix approach. Both unrestricted order matrices and matrices in which it was assumed that the headgroups execute axially symmetric motions were used. Both approaches led to nearly the same averaged headgroup orientation for each glycoside. Where the data were sufficient in quality and/or quantity, the unrestricted approach allowed the anisotropy of motion to be defined. The orientations observed for each glycoside were found to be consistent with a model previously suggested to account for the observed structure of β-dodecyl glucopyranoside at a bilayer interface (Sanders, C. R.; Prestegard, J. H. *J. Am. Chem. Soc.* **1991**, *113*, 1987-1996). These results suggest that, despite the energetic complexity of membrane interfaces, it may be possible to make reasonable predictions about the interfacial structures of amphiphiles based on consideration of the topological placement of hydrophobic/hydrophilic moieties within the molecule.

Introduction

A wide variety of cellular functions are mediated by interactions at the surfaces of membranes.[1-3] While the conformational properties of molecules involved in these interactions are of obvious importance, their study at the surfaces of membranes has been difficult. Many physical investigations have, therefore, focused on the conformational properties of solubilized membrane receptors or receptor fragments.[4-8] Such studies have provided a useful basis for future studies. Yet, it must be realized that the proximity of the membrane surfaces may alter or refine the presentation of receptors in their native environments.

Glycolipids are one simple class of membrane receptors whose properties have begun to be studied in both solution and membrane phases.[4-15] Recently, we presented a preliminary study of one glycolipid in an effort to illustrate some new methodology which may be applicable to receptor conformation in membranelike environments and introduced a simple model to account for the structure observed.[16] The headgroup of β-dodecyl glucopyranoside (BDOG) in bilayers of an oriented dimyristoylphosphatidylcholine (DMPC)-detergent system was the subject of that study. The methodology employed liquid crystalline (LC) NMR methods and a complete order matrix analysis.

A slightly revised version of the orientation of the headgroup of BDOG in the principle order frame is shown in Figure 8A. If the *z* axis is taken to be coincident with the bilayer normal, the 2 and 6 carbons form a line which is approximately parallel to the plane of the bilayer, and the glucose ring extends almost fully along the bilayer normal. Rotation is found to be more restricted about the *x* order axis than about the *y* order axis. It was suggested that the observed structure and motional asymmetry for BDOG could be rationalized by considering the hydrophilic/hydrophobic properties of groups on the sugar ring and their likely interactions with the hydrophobic core of the membrane. Extension of the entire ring away from the interface obviously helps to reduce polar/hydrophobic interactions with many of the substituent hydroxyl groups. The observed asymmetry of motion can be rationalized because rotations about the less hindered *y* axis do not readily result in insertion of 2- or 6-position hydroxyls into the interface, whereas rotations about *x* will result in increased interactions between the hydrophobic region of the interface and the polar 2 or 6 substituents.

While the proposed model accounting for the structure of BDOG is attractive, it is based upon the study of a single molecule and on an incomplete investigation of the assumption that the liquid crystal environment mimics more readily accepted models of phospholipid bilayers. In particular, any possible direct effect of a detergent 3-[(3-cholamidopropyl)dimethylammonio]-2-hydroxy-1-propanesulfonate (CHAPSO), present in the liquid crystal preparation, should be explored. The dominant morphology in the orientable CHAPSO-DMPC mixtures used in our previous study is thought to be discoidal bilayer fragments whose edges are stabilized by the CHAPSO.[17,18] These disks interact cooperatively in the presence of a strong magnetic field to orient with their bilayer normals orthogonal to the field direction. Because the bilayers maintain many of the characteristic qualities of pure

† Present address: Department of Physiology and Biophysics, Case Western Reserve University.

(1) Gennis, R. B. *Biomembranes*; Springer-Verlag: New York, 1989.
(2) Bock, G., Harnett, S., Eds. *Carbohydrate Recognition and Cellular Function*; *Ciba Found. Symp.* **1989**, 145.
(3) Curatolo, W. *Biochim. Biophys. Acta* **1987**, *906*, 137-160.
(4) Sabesan, S.; Duus, J.; Flukunaga, T.; Bock, K.; Ludvigsen, S. *J. Am. Chem. Soc.* **1991**, *113*, 3336-3346.
(5) Scarsdale, J. N.; Prestegard, J. H.; Yu, R. K. *Biochemistry* **1990**, *29*, 9843-9855.
(6) Acquotti, D.; Poppe, L.; Dabrowski, J.; von der Lieth, C.-W.; Sonnino, S.; Tettamanti, G. *J. Am. Chem. Soc.* **1990**, *112*, 7772-7778.
(7) Poppe, L.; von der Lieth, C.-W.; Dabrowski, J. *J. Am. Chem. Soc.* **1990**, *112*, 7762-7771.
(8) Homans, S. W. *Prog. Nucl. Magn. Reson. Spectrosc.* **1990**, *22*, 55-81.
(9) Winsborrow, B. G.; Smith, I. C. P.; Jarrell, H. C. *Biophys. J.* **1991**, *59*, 729-741.
(10) Speyer, J. B.; Weber, R. T.; Das Gupta, S. K.; Griffin, R. G. *Biochemistry* **1989**, *28*, 9569-9574.
(11) Skarjune, R.; Oldfield, E. *Biochemistry* **1982**, *21*, 3154-3160.
(12) Ram, P.; Prestegard, J. H. *J. Am. Chem. Soc.* **1988**, *110*, 2383-2388.
(13) Sen, A.; Hui, S.-W.; Mannock, D. A.; Lewis, R. N. A. H.; McElhaney, R. N. *Biochemistry* **1990**, *29*, 7800-7804.
(14) Lewis, R. N. A. H.; Mannock, D. A.; McElhaney, R. N.; Wong, P. T. T.; Mantsch, H. M. *Biochemistry* **1990**, *29*, 8933-8943.
(15) Curatolo, W. *Biochim. Biophys. Acta* **1987**, *906*, 111-136.
(16) Sanders, C. R.; Prestegard, J. H. *J. Am. Chem. Soc.* **1991**, *113*, 1987-1996. It should be noted that there are two significant errors in this paper. First, eq 2 has an extra factor of 2. Second, the labels for the *x* and *y* order axes in Figure 9 are reversed.
(17) Sanders, C. R.; Prestegard, J. H. *Biophys. J.* **1990**, *58*, 447-460.
(18) Muller, K. *Biochemistry* **1981**, *20*, 404-414.

0002-7863/92/1514-7096$03.00/0

phospholipid membranes, this system seems attractive for widespread use as a model membrane system. However, the level of CHAPSO present is substantial and, to some extent, could affect the interior of the disks as well the edges. Other possible obstacles confronting straightforward interpretation of the structure of BDOG include the possibility that interglycoside interactions may influence conformations and the well-known complexity of bilayer interfaces.[19]

In this contribution, we attempt to address some of the shortcomings mentioned above. First, in order to help sort out any spurious effects induced by CHAPSO and interglycoside interactions, a number of control experiments are presented. Second, the validity of our proposal for the physical significance of the structure of BDOG is examined by systematically removing the 2- or 6-hydroxyls to create a more hydrophobic (methyl or methylene) headgroup surface. If the previous suggestions are correct, the average orientation of the glucopyranose ring should be altered to optimize hydrophobic interactions between the membrane and the newly exposed hydrocarbon and to minimize unfavorable interactions of the remaining hydroxyls. When the covalent structure at the solvent-exposed end of the glucose ring is perturbed, this should show little effect on the overall orientation. We have therefore synthesized ^{13}C labeled β-dodecyl 6-deoxyglucopyranoside, β-tetradecyl 2-deoxyglucopyranoside, and β-dodecyl galactopyranoside and have determined their interfacial orientations. Structures with a slightly wider array of modifications have also been synthesized and examined. These include α-dodecyl glucopyranoside, α-tetradecyl 2-deoxyglucopyranoside, α-tetradecyl 2,3-dideoxyglucopyranoside, and α-tetradecyl 2,3-dideoxy-*erythro*-hex-2-enopyranoside.

In addition to addressing the above issues, this work is of some methodological significance. Many previous solid-state NMR studies of membrane components have relied upon the assumption that the molecule under observation executes motional deviations about the bilayer normal which are axially symmetric.[11,12,20] It has not been clear what effect the failure of this assumption would have upon the accuracy of average structures determined. In our previous study of BDOG we observed that despite the fact that motions are *not* truly symmetric, there is little difference in the average interfacial headgroup orientation determined using a complete order matrix approach and using an axial symmetry assumption. The number of different structures addressed in this paper presents the opportunity to examine this issue in more detail.

The study of BDOG also relied solely upon dipolar and quadrupolar coupling NMR measurements to provide data which can be interpreted in terms of an order matrix. ^{13}C chemical shift anisotropy (CSA) tensors offer a similar geometric dependence and have been effectively employed in structural studies of other classes of membrane-associated molecules.[21-24] CSA tensors have been determined for some carbohydrates,[25,26] which can serve as models in studies of related alkyl glycosides. We have therefore attempted to include these data in the current study.

Finally, it should be noted that the structures under examination bear a close relationship to the alkyl glycoside detergents. These mild surfactants are now finding widespread application in biomembrane-related research.[27-30] Structural data will hopefully illuminate the properties of this class of amphiphiles and their interactions with membranes.

Materials and Methods

Syntheses. Chemicals used as starting materials and most biochemicals used in sample preparation were purchased from either Aldrich (Milwaukee, WI) or Sigma (St. Louis, MO). [$^{13}C_6$]Glucose (various levels of labeling) was obtained from both MSD (Montreal, Canada) and Cambridge Isotopes (Woburn, MA), [$^{13}C_6$]galactose (20% enrichment) was obtained from the latter source. Dowex 50W-X4 (H^+) was purchased from BioRad (Richmond, CA), rinsed with methanol, and dried in a desiccator before use. The following solvent systems were utilized in running thin layer chromatography (TLC, 60 μm silica) or flash chromatography (40 μm silica): I, 5:1 chloroform:methanol; II, 7:1 chloroform:methanol; III, 4:1 hexane:ethyl acetate; IV, 3:1 hexane:ethyl acetate. An aqueous 10% sulfuric acid, 10% ammonium molybdate, 1% ceric sulfate stain was used to visualize TLC plates.

A. β-Hexyl Glucopyranoside, β-Dodecyl [$^{13}C_6$]Glucopyranoside, and β-Dodecyl Galactopyranoside. These compounds were synthesized as described previously for BDOG,[16,31] using $AgCO_3$ in the presence of I_2 and molecular sieves to catalyze the glycosylation of the appropriate tetraacetylglycopyranosyl bromide. Products were isolated essentially as described for BDOG and were identified and judged to be >90% pure by both ^1H and ^{13}C NMR.

B. β-Dodecyl [$^{13}C_6$]-6-Deoxyglucopyranoside. Tosyl chloride was recrystallized from petroleum ether and dried in vacuo over P_2O_5 prior to the following usage: 23 mg of labeled BDOG was mixed with 25 mg of tosyl chloride, dissolved by 1 mL of dry pyridine, and stirred at room temperature in the dark and under dry argon for 2 days. TLC of the now pink reaction mixture indicated that conversion of BDOG (R_f in I = 0.420) to the product (R_f = 0.73) was essentially complete. A few milliliters of methanol were added to the mixture to cease reaction, and after drying, the product was isolated by flash chromatography using solvent system II at a total yield of 75%. The 24 mg of β-dodecyl 6-tosylglucopyranoside was dissolved by 1.5 mL of dry tetrahydrofuran (THF) and added to a stirred mixture of 15 mg of $LiAlH_4$ and 0.5 mL of THF under argon at room temperature. The reaction was allowed to proceed for 24 h and was observed to be complete by TLC (R_f of major product in II = 0.475). A little water was carefully added to quench the remaining hydride, and 2 N NaOH was added to help coagulate the pasty suspension. The solid was filtered out (with much effort) and rinsed with methanol. The filtrate was rotary evaporated to dryness and flash chromatographed using solvent system II. The desired product was separated from the slower running side product (β-dodecyl glucoside) in a yield from the tosylate of 24%. ^{13}C NMR (in CH_3OD) confirmed the identity of the product as the desired 6-deoxyglycoside.[32]

C. α-Dodecyl [$^{13}C_6$]Glucopyranoside. Direct Fisher glycosylation of glucose was accomplished by refluxing a mixture of 85 mg of labeled glucose, 0.25 mL of dodecanol, and 25 mg of Dowex 50W-X4 (H^+ form) in 4 mL of dimethoxyethane for 1 h, at which point another 25 mg of Dowex was added, followed by reflux for another hour. The latter step was repeated to bring the total reaction time to 3 h. TLC (system II) demonstrated the presence of some dodecyl glucoside product (R_f = 0.325), and the mixture was cooled. The Dowex and undissolved glucose were filtered out, and the product pool was dried and flash chromatographed using solvent system II. Fractions containing the product were dried and found to be a ca. 2:1 mixture of α- and β-dodecyl glucopyranoside by ^1H NMR (yield of only 5% because of the insolubility of the starting glucose). In order to separate the anomers, the 8 mg of mixed anomers was acetylated by being stirred in 2 mL of pyridine and 0.5 mL of acetic anhydride overnight, followed by removal of the pyridine, acetic acid, and anhydride in vacuo. Flash chromatography (solvent system III) cleanly resolved the α anomer (R_f = 0.24) from the β anomer (R_f = 0.22). The dried product was dissolved by 2 mL of methanol and deacetylated by adding 0.025 mL of 1 M Na^+OMe^- at room temperature followed by the addition of 35 mg of Dowex X4 (H^+) and filtration. The filtrate was dried to yield 3 mg of 90% pure α-dodecyl glucopyranoside as judged by ^{13}C NMR.[33]

D. α-Dodecyl [$^{13}C_6$]-2,3-Dideoxy-*erythro*-hex-2-enopyranoside. Labeled glucose was acetylated and brominated[31] and then converted to 3,4,6-triacetyl glucal by reaction with Zn in acetic acid.[34] After filtering out the solid, the aqueous acetic acid solution was extracted repeatedly with chloroform, saving the nonpolar layer each time. The organic phase was then extracted with water (2×), saturated $NaHCO_3$ (2×), and water

(19) Cevc, G. *Biochim. Biophys. Acta* **1990**, *1031*, 311-382.
(20) Jarrell, H. C.; Jovall, P. A.; Giziewicz, J. B.; Turner, L. A.; Smith, I. C. P. *Biochemistry* **1987**, *26*, 1805-1811.
(21) Seelig, J. *Biochim. Biophys. Acta* **1978**, *515*, 105-140.
(22) Shen, K.-J.; Kim, Y.; Colnago, L. A.; Opella, S. J. *Science* **1991**, *252*, 1303-1305.
(23) Nicholson, L. K.; Teng, Q.; Cross, T. A. *J. Mol. Biol.* **1991**, *218*, 621-637.
(24) Cornell, B. A.; Separovic, F.; Baldassi, A. J.; Smith, R. *Biophys. J.* **1988**, *53*, 67-76.
(25) McDowell, C. A.; Naito, A.; Sastry, D. L.; Takegoshi, K. *J. Magn. Reson.* **1988**, *78*, 494-510.
(26) Sastry, D. L.; Takegoshi, K.; McDowell, C. A. *Carbohydr. Res.* **1987**, *165*, 161-171.
(27) Milligan, D.; Koshland, D. *J. Biol. Chem.* **1990**, *265*, 4455-4460.
(28) Davidson, A.; Nikaido, H. *J. Biol. Chem.* **1990**, *265*, 4254-4260.
(29) Parries, G. S.; Hokin-Neaverson, M. *Biochemistry* **1984**, *23*, 4785-4791.
(30) Ueno, M. *Biochemistry* **1989**, *28*, 5631-5634.
(31) Rosevear, P.; Van Aken, T.; Baxter, J.; Ferguson-Miller, S. *Biochemistry* **1980**, *19*, 4108-4115.
(32) Gorin, P. J.; Mazurek, M. *Can. J. Chem.* **1975**, *53*, 1212-1223.
(33) Bock, K.; Thogersen, H. *Annu. Rep. NMR. Spectrosc.* **1982**, *13*, 1-57.
(34) Kozikowski, A. P.; Lee, J. *J. Org. Chem.* **1990**, *55*, 863-870.

(3×), followed by drying with $MgSO_4$, filtration, rotary evaporation, and additional drying in vacuo to produce the labeled triacetyl glucal in a yield of about 80% from the starting glucose. The triacetylglucal (0.21 g) was dissolved in 2 mL of 1,2-dichloroethane and 0.25 mL of dodecanol was added. TLC (solvent system IV) showed R_f values for the starting glucal and alcohol to be 0.33 and 0.52. To this mixture was added 50 mg of Dowex 50W-X4 (H^+), and refluxing was commenced. The Dowex turned black within minutes, and the mixture was allowed to cool. TLC indicated that most of the glucal had been converted into a major product with R_f (solvent system IV) = 0.67 and a minor product of R_f = 0.62. The Dowex was filtered out, and the solution was rotary evaporated and flash chromatographed on a column eluted by 10:1 hexane:ethyl acetate. Pure fractions containing the major product were pooled to produce a white solid weighing 105 mg. ^1H NMR in $CDCl_3$ indicated that the expected acid-catalyzed allylic rearrangement (known as the Ferrier reaction) had occurred, yielding α-dodecyl 4,6-diacetyl-2,3-dideoxy-*erythro*-hex-2-enopyranoside.[35,37] This compound was deprotected by dissolution in 3 mL of methanol, addition of 0.05 mL of 1M sodium methoxide, and stirring for 2 h at room temperature. The methoxide was neutralized by adding methanol-washed Dowex 50W-X4 (H^+), followed by filtration and rotary evaporation of the filtrate to produce 80 mg of a white powder. The identity of this product was confirmed as α-dodecyl [$^{13}C_6$]-2,3-dideoxy-*erythro*-hex-2-enopyranoside by both single quantum and double quantum filtered (INADEQUATE) ^{13}C NMR in CH_3OD.

E. α-Dodecyl [$^{13}C_6$]-2,3-Dideoxyglucopyranoside. The above α-2,3 unsaturated 2,3-dideoxyglucoside (20 mg) was mixed with 25 mg of 10% Pd/C in 2 mL of ethanol and stirred at room temperature under a hydrogen balloon for 12 h. TLC showed only a spot possessing the same R_f as the starting alkene. However, after staining and heating, this spot developed very slowly to produce a greenish-blue color, in contrast to the starting material, which develops a dark blue color almost immediately after commencement of heating. Most of the Pd/C was filtered out, and the ethanolic solution was evaporated and flash chromatographed (solvent system II) to produce a white solid weighing 17 mg (85% yield). ^{13}C NMR confirmed its identity as >90% pure labeled α-dodecyl 2,3-dideoxyglucoside. (^{13}C sugar resonances in CH_3OD: C1, 96.7; C2, C3, 29.5, 29.3; C4, C5, 74.3, 66.5; C6, 62.2).

F. α- and β-Tetradecyl [$^{13}C_6$]-2-Deoxyglucopyranoside. Labeled 3,4,6-triacetyl glucal (50 mg) was dissolved in 1 mL of methylene chloride and stirred over a −15 °C ethylene glycol dry ice bath. Br_2 was then dropped slowly into the solution until the distinctive color of the halogen persisted. The solution was rotary evaporated and dried further in vacuo. The residue was dissolved by 1 mL of 1,2-dichloroethane and then mixed with 150 mg of activated 4-Å powdered molecular sieves, 50 mg of $HgBr_2$, and 50 mg of tetradecanol on ice under dry argon. After being stirred for 20 min the reaction mixture was allowed to warm to room temperature and react for another 8 h. TLC (solvent system IV) showed the appearance of three products having R_f values of 0.78, 0.74, and 0.65. These three products were purified by flash chromatography eluting with 10:1 hexane:ethyl acetate. The three pools were dried to yield products in amounts (in order from high to low R_f) of 24, 21, and 17 mg, respectively. Each product was then dissolved in 1.5 mL of tetrahydrofuran and stirred on ice, under dry Ar, during the addition of 30 mg of $LiAlH_4$. Each mixture was then refluxed under Ar for 7 h. Reactions were terminated by carefully adding methanol until no additional evolution of hydrogen gas was observed. This was followed by the addition to each of 200 mg of Dowex 50W-X4 (H^+) and about 8 mL of THF. The mixtures were then filtered and the solids rinsed with EtOH. TLC analysis of the filtrates (solvent system II) showed only a single product in each case (R_f of 0.41). ^{13}C NMR indicated that the high and medium R_f pool glycosylation products led to the same (>90% pure) product in ca. 46% yield from the acetylated, 2-brominated glycoside. This product is α-tetradecyl 2-deoxyglucopyranoside.[38] The differing R_f values of the two acetylated, brominated glycosylation intermediates giving rise to α product are likely to originate in the identities of the intermediates as axial and equatorial 2-Br glycosides. The low-R_f product of the glycosylation reaction led to >90% pure β-tetradecyl 2-deoxyglucopyranoside in a ca. 25% yield as confirmed by ^{13}C NMR.[38] The overall yields of the α and β anomers from the starting glucal were 20% and 4%, respectively.

Sample Preparation and NMR Methods. Liquid crystalline NMR samples were prepared directly in 5 mm diameter NMR tubes. First, the desired quantity of the alkyl glycoside dissolved in methanol was added to the tube, cooled, and evaporated in vacuo. The appropriate amounts of DMPC, CHAPSO, and 0.1M KCl in D_2O were then added. A buffer was deemed unnecessary because all of the species in our samples were neutral or zwitterionic. The sample was sealed with teflon tape, capped, and mixed to homogeneity using a combination of centrifugation, heating, cooling, and sonication. The 1:3 CHAPSO:DMPC samples typically utilized in this study are normally viscous and clear above room temperature and are fluid and clear between room temperature and about 10 °C. Below this, they become cloudy. Samples were cooled on ice before insertion into the spectrometer magnet with probe temperature at 40°.

All spectra were acquired using a Bruker AM-500 NMR spectrometer. ^{13}C NMR (125.76 MHz) spectra were acquired with a standard 5-mm $^{13}C/^1H$ "dual" probe. ^{31}P NMR spectra were obtained using a broadband multinuclear 5-mm inverse probe. Spectra were acquired unlocked and without sample spinning. ^1H decoupling was effected using a WALTZ modulation scheme[39] and a high (40 watts) decoupling power setting. Because of sample heating, which can potentially occur using such high decoupling power, care was taken to keep the acquisition time less than 0.1 s while maintaining a fixed delay between scans of at least 1.5 s. Additional details of the NMR methods used can be found in our previous contribution[16] and in the figure legends.

Theory and Calculations. A. Dipolar Coupling. Dipolar coupling between proximate spin $^1/_2$ nuclei is known to be dependent on both internuclear distance (r^{-3}) and the angle of the vector between coupled spins and the applied magnetic field. In isotropic solution, this coupling is averaged to zero by molecular reorientation. In liquid crystal media, averaging still occurs but leads to a scaling of dipolar coupling rather than elimination. In the case of the system composed of CHAPSO–DMPC discoidal micelles, the orientational averaging comes from several sources. First, the assembly itself is free to move within bounds defined by the liquid crystal environment. Because of the anisotropy of the diamagnetic susceptibility of the phosphatidylcholine bilayer, discoids tend to orient with the bilayer normal 90° with respect to the magnetic field[17] and the discoids tend to wobble about this orientation. Second, the component molecules appear to undergo motional deviations about the normal of an individual bilayer fragment, which include both rotation and oscillation. The latter rotation and oscillation should be directly comparable to that observed in other model membrane preparations including multilayer dispersions of pure phospholipids. The effects of the 90° orientation and additional wobble introduced by the finite size of the micellar disks are, however, unique to our system and can be represented by a separate order parameter, $S_{micelle}$. This order parameter affects all molecules equally making it convenient to separate and treat independently of reductions in order that arise from molecular motions within the bilayer. The further reduction in order for vectors defined within individual molecules is then represented by an additional factor $\langle(3\cos^2\theta - 1)/2\rangle$, and overall dipolar coupling can be expressed as:

$$D_{ij} = -\frac{\gamma_i\gamma_j h}{2\pi^2 r^3} S_{micelle} \left\langle \frac{3\cos^2\theta - 1}{2} \right\rangle \quad (1)$$

Here the γ_{ij} are the magnetogyric ratios for the interacting spin $^1/_2$ nuclei, h is Planck's constant, r is the internuclear distance, and θ is the angle of the internuclear vector with respect to principal axis of motional averaging: the bilayer normal.

Because $S_{micelle}$ behaves as a common scaling factor for all measured dipolar couplings, it is only important if one wishes to quantitate the amplitudes of motion as opposed to qualitatively characterizing the geometry and asymmetry of motion. It can, however, be estimated from measurements on the phospholipids which compose the bulk of the bilayer matrix. Both deuterium quadrupole splittings of perdeuterated lipids and chemical shift anisotropy offsets of resonances in ^{31}P NMR spectra offer opportunities to do this and give similar results.[40] For the ^{31}P case, $S_{micelle}$ can be calculated using the following formula:

$$S_{micelle} = \frac{\sigma_{obsd} - \sigma_{iso}}{\sigma_{0°} - \sigma_{iso}} \quad (2)$$

$\sigma_{0°}$, the chemical shift for an ideal bilayer with its normal parallel to the applied field, was obtained from the downfield edge of a ^{31}P powder pattern from an aqueous DMPC dispersion at 40°, and σ_{iso} was obtained either from the geometric center of this pattern or the chemical shift of the signal from DMPC in spherical micelles (CHAPSO:DMPC ratio (mol/mol) greater than 1:2). σ_{obsd} is simply the observed shift of the single line in an oriented discoidal phase. For samples with DMPC:CHAPSO ratios of 3:1, $S_{micelle}$ was observed to be −0.25, with a factor of −0.5 coming from the 90° orientation and another 0.5 arising from

(35) Baer, H. H.; Hanna, Z. S. *Can. J. Chem.* **1981**, *59*, 889–906.
(36) Fraser-Reid, B.; Iley, D. E. *Can. J. Chem.* **1979**, *57*, 645–652.
(37) Ferrier, R. J. *Carbohydr.: Chem. Biochem.* **1969**, *24*, 199–266.
(38) Bock, K.; Pedersen, C. *J. Chem. Soc., Perkins Trans. 2* **1974**, 293–297.
(39) Shaka, A. J.; Keeler, J.; Freeman, R. J. *J. Magn. Reson.* **1983**, *53*, 313–340.
(40) Sanders, C. R.; Schaff, J.; Prestegard, J. H., manuscript in preparation.

discoidal assembly motions. Defining $S_{micelle}$ in this way allows the additional averaging of eq 1 to be compared directly to results from previous studies on order in multilayer dispersions of phospholipids.

An established way to express the additional angular average term arising from internal motions in eq 1 lies in the use of an order matrix.[41-43] In a Cartesian system nine elements are used to describe the averaging of axes of an arbitrary molecule fixed system with respect to a director axis. Because $S(i,j) = S(j,i)$ and because the matrix is traceless, only five of these are independent. These elements are defined as:

$$S(i,j) = \left\langle \frac{3\cos\rho_i\cos\rho_j - \delta_{i,j}}{2} \right\rangle \quad (3)$$

where the ρ define the angle made by the i or j molecular axis relative to the principle axis (i.e., the bilayer normal) and δ is 1 for $i = j$ and 0 otherwise. The term expressing averaging of the angular-dependent interaction in this arbitrary molecular axis system can then be given as follows:[41,42]

$$\left\langle \frac{3\cos^2\theta - 1}{2} \right\rangle = (\cos^2\phi_x)(-S(y,y) - S(z,z)) + (\cos^2\phi_y)S(y,y) + (\cos^2\phi_z)S(z,z) + 2(\cos\phi_x\cos\phi_y)S(x,y) + 2(\cos\phi_x\cos\phi_z)S(x,z) + 2(\cos\phi_y\cos\phi_z)S(y,z) \quad (4)$$

where ϕ_i is the angle of the internuclear vector relative to the i molecular axis.

The order matrix can be diagonalized by transforming from an arbitrary molecular axis system to a principle axis system. The direction of maximum order in this system is taken to be the z (director) axis. For a bilayer system, it is reasonable to assume this direction of maximum order to be coincident with the bilayer normal. The eigenvectors corresponding to the eigenvalues (new order parameters: $S_{x'}$, $S_{y'}$, and $S_{z'}$) then give the direction of the bilayer normal and the new x' and y' order axes in the original molecular frame.

The eigenvectors associated with the x, y, and z order axes also form the columns of a rotation matrix that can be interpreted in terms of Euler rotations which transform the molecular frame to the new principle order frame. Thus, the Euler angles describing the orientation of the molecular frame can easily be determined. In this paper, the convention of Goldstein[44] for the Euler angles is used except that the present use of β, α, and γ corresponds to his θ, ϕ, and ψ.

Previous analyses of lipid bilayer data often assume axial symmetry. Equation 4 can be simplified to treat this case if we assume that we can initially choose a molecular frame that coincides with the order frame and set $S_y = S_x$. If the order frame and the molecular frame are coincident, then only the $S(i,i)$ terms in eq 4 survive. With $S_y = S_x$, eq 4 is reduced to

$$S_z(\cos^2\phi_z - 0.5(\cos^2\phi_y + \cos^2\phi_x)) \quad (5)$$

Since the sum of the squares of a set of direction cosines is equal to 1, eq 5 can be reduced to

$$S_z\left(\frac{3\cos^2\phi_z - 1}{2}\right) \quad (6)$$

This equation can then be substituted back into eq 1 in place of the internal angular average term to produce the usual expression for reduction of dipolar (or quadrupolar) splittings in an axially symmetric system. In these systems, only a single molecular order term appears along with a geometric factor relating a dipolar vector to the principle order axis. If it is not possible to pick a molecular frame coincident with the order frame initially, ϕ_z in eq 6 can be related to direction cosines of the vector in any arbitrary molecular Cartesian frame using the Euler rotations β and γ:

$$\cos\phi = \cos\beta\cos(z) + \sin\beta\cos\gamma\cos(y) + \sin\beta\sin\gamma\cos(x) \quad (7)$$

In this case, an experimental splitting will be dependent upon three unknowns β, γ, and S_z.

B. Chemical Shift Anisotropy. The observed chemical shift in an anisotropic system shows a dependence on order and molecular orientation which is very similar to that for the dipolar coupling described above. Chemical shift can be described as the sum of isotropic and anisotropic parts:

$$\sigma_{obsd} = \tfrac{1}{3}(\sigma_{11} + \sigma_{22} + \sigma_{33}) + \tfrac{2}{3}\sigma_{an} \quad (8)$$

In a mobile system σ_{an} is an average of the deviations in the chemical shift from its isotropic value and can be described using a treatment similar to that for dipolar coupling.[41,42]

$$\langle\sigma_{an}\rangle = S_{micelle}[\sum_{i,j} S(i,j)\sigma'_{i,j}] \quad (9)$$

Here $S(i,j)$ are elements of the order matrix in an arbitrary molecular frame, and the $\sigma'_{i,j}$ are the elements of the chemical shift tensor expressed in that frame. $S_{micelle}$ can be estimated as described above (eq 2), and σ'_{ij} can be found by simple orthogonal transformation from the principle frame of the shift tensor to the (arbitrary) molecular frame of a sugar ring. Once this is done, the observed σ_{an}, like dipolar coupling, is dependent upon five independent order matrix elements.

C. Calculations. A FORTRAN program (ORDERTEN) was previously described[16] for searching for elements of the order matrix which agree with experimental observation. Diagonalization of these matrices yields S_i and the orientation of the molecular segment in question. This program has been refined somewhat since our original report. It now allows direct entering of experimental data and employs a data weighing method based upon experimental uncertainty. In addition to direct output of order tensor elements, Euler angles describing the relationship of an initial molecular frame to the bilayer director frame are calculated. It is also possible to limit a search to parameters that pertain to an axially symmetric case (eqs 6 and 7). Furthermore, if any chemical shift tensors are known for moieties within the molecule of interest, the program will take principal CSA tensor values, together with information defining their orientation with respect to a molecular frame, and calculate σ_{an} for each acceptable order matrix solution. Comparison of these calculated values with experimentally observed chemical shift values potentially provides a useful means of screening solutions.

In order to improve the previous[16] treatment of experimental error, dipolar data were assigned relative weights within the program that were proportional to the ratio of the maximum expected splitting for a pair of nuclei and the experimentally observed uncertainty ($\Delta\nu$).

$$\text{weight} = \frac{\gamma_i\gamma_j}{2\pi^2 r^3\Delta\nu} \quad (10)$$

For the purpose of calculation, it was assumed that the glycopyranoside rings were fixed in their $^4C_1$ chair conformations with the population of higher energy conformers being too small to influence the NMR data. Failure of this assumption should be manifested as an inability to obtain a solution for the experimental data due to r^{-3} being different than assumed and due to changes in the relative internal orientations of internuclear vectors. As will be described, such failures to find solutions were not encountered.

Starting structures were generated using the molecular modeling package AMBER[45,46] and then rotated and translated to bring them into a common right-handed molecular frame. We utilized a frame which has its origin at the midpoint of a vector between the 1 and 4 glycosyl carbons and the positive z axis running through carbon C4. The positive x axis was chosen to intersect the C2-C3 bond. This places the y axis normal to the approximate plane of the entire sugar ring.

Results

Control Experiments on β-Dodecyl Glucoside. A. BDOG in DMPC Liposomes. Before proceeding to analysis of new structures we return briefly to BDOG in an effort to ensure that no system artifacts play a role in defining its observed interfacial structure. One test stems from comparison of data from the oriented CHAPSO-DMPC system to data from nonoriented DMPC multilayers. The 1-D proton decoupled ^{13}C NMR spectrum arising from an unoriented DMPC liposome sample containing [$^{13}C_6$]BDOG (66% $^{13}C_6$) is shown in Figure 1. As expected, the resonances are somewhat asymmetric and broad because of powder pattern CSA and dipolar coupling effects. The characteristic features of a ^{13}C-^{13}C dipolar powder pattern are not easily observed because of its small width and because of the superposition of spectra from 34% single-labeled sites. However, crosspeaks in a double quantum filtered (DQF) COSY[47] spectrum (Figure

(41) Saupe, A. *Angew. Chem., Int. Ed. Engl.* **1968**, *7*, 97-112.
(42) Diehl, P.; Khetrepal, C. L. *NMR: Basic Princ. Prog.* **1969**, *1*, 1-95.
(43) Emsley, J. W., Ed. *NMR of Liquid Crystals*; Reidel: Dordrect, 1985.
(44) Goldstein, H. *Classical Mechanics*; Addison-Wesley: Cambridge, 1953.
(45) Weiner, P. K.; Singh, U. C.; Kollman, P. A.; Caldwell, J.; Case, D. A. AMBER. Version 3.0. University of California, San Francisco, 1986.
(46) Weiner, P. K.; Kollman, P. A. *J. Comput. Chem.* **1981**, *2*, 287-303.
(47) Marion, D.; Wuthrich, K. *Biochem. Biophys. Res. Commun.* **1983**, *113*, 967-974.

Table I. Comparison of Dipolar Coupling Constants Measured[a] for β-Glucosides in Various Phospholipid Media[b] at 40 °C

vector	BDOG in 1:3 CHAPSO:DMPC[c]	BDOG in pure DMPC[d] obsd	BDOG in pure DMPC[d] cor	BDOG in 1:4.85 CHAPSO:DMPC[e] obsd	BDOG in 1:4.85 CHAPSO:DMPC[e] cor	BDOG in 1:3 Triton:DMPC[f] obsd	BDOG in 1:3 Triton:DMPC[f] cor	β-hexyl glucoside in 1:3 CHAPSO:DMPC[g] obsd	β-hexyl glucoside in 1:3 CHAPSO:DMPC[g] cor
C1–C2	220 ± 15	|340 ± 80|	149	|385 ± 40|	228	|403 ± 60|	180	|250 ± 50|	139
C1–C3	100 ± 25			|187 ± 30|	125	|171 ± 30|	86	|86 ± 30|	58
C1–H1	−1420 ± 200	|2700 ± 700|	−1440	|1400 ± 200|	−1030	|2000 ± 200|	−1085	|550 ± 100|	−720
C5–C6	−219 ± 15	|282 ± 80|	−162	|295 ± 35|	−225	|391 ± 20|	−216	|146 ± 10|	−126
C4–C6	0 ± 20					0 ± 15	0	0 ± 15	0
C4–C5	265 ± 25			|450 ± 40|	275				
C3–C4	−225 ± 20					|294 ± 50|	−168	|150 ± 30|	−129

[a] The "corrected" values were produced for use in checking for consistency with the data in the first column. The observed coupling was assigned the same sign as the coupling from column 1 and from this was subtracted J (+42 for carbon–carbon splittings, +170 for carbon–proton), and then this was multiplied by the factor which results from dividing the $S_{micelle}$ of the standard 1:3, 30% sample (−0.25) by the $S_{micelle}$ for the sample giving rise to the observed coupling. [b] The samples in all cases contained 30% (w/v) total amphiphile in 0.1 M KCl in D_2O. [c] These data are from our earlier report ($S_{micelle}$ = −0.25). [d] $S_{micelle}$ = −0.5. [e] $S_{micelle}$ = −0.375. [f] $S_{micelle}$ = −0.5. [g] $S_{micelle}$ = −0.375.

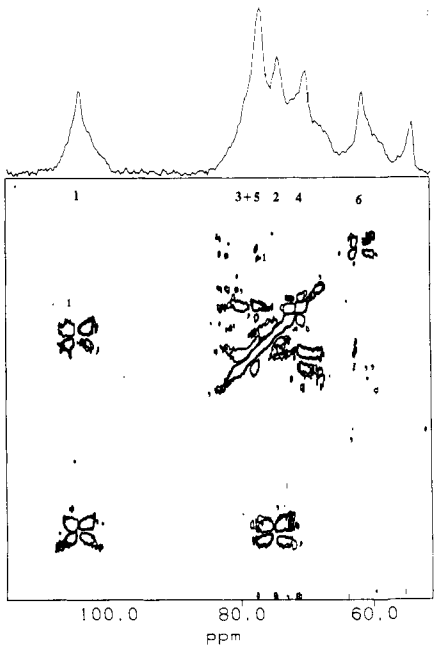

Figure 1. 1-D and double quantum filtered ^{13}C–^{13}C COSY (proton-decoupled) spectra of a 0.31-mL sample containing β-dodecyl [$^{13}C_6$]-glucopyranoside (66% $^{13}C_6$) in an unoriented 40 °C DMPC dispersion (BDOG:DMPC = 1:5.2, mol/mol). The total lipid concentration was 30% (w/v) in 0.1 M KCl and D_2O. 80 $t1$ points were acquired with 592 scans per point, 1024 points in $f2$, and a scan recycling time of 1.75 s. The sweep width in both dimensions was 8000 Hz.

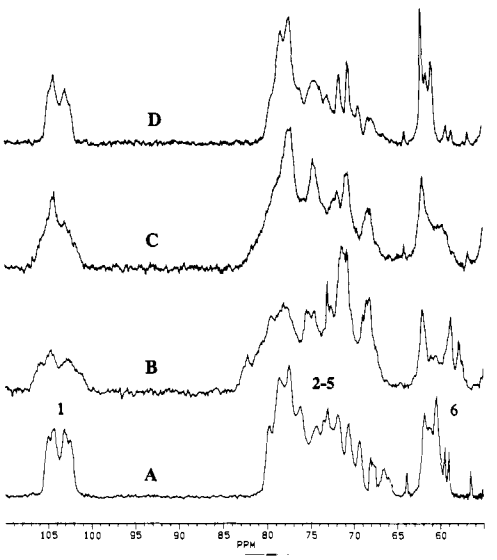

Figure 2. Proton-decoupled ^{13}C NMR spectra of headgroup-labeled β-dodecyl or hexyl glucoside (66% $^{13}C_6$) in various 40 °C DMPC environments. (A) "Standard" 1:3 CHAPSO:DMPC mixture (BDOG:DMPC = 1:5.6); (B) 1:3 Triton X-100:DMPC (BDOG:DMPC = 1:11.9); (C) 1:4.85 CHAPSO:DMPC (BDOG:DMPC = 1:5.9); (D) 1:5 CHAPSO:DMPC (β-hexyl glucoside:DMPC = 1:7.1). In all cases the total lipid was 30% (w/v) in 0.1 M KCl in D_2O. Only the sugar carbon spectral regions are shown.

1) select for double-labeled sites and contain dipolar powder pattern information. Splittings, while heterogeneous, are dominated by the 90° powder component which can be associated with the measured splitting. From observed crosspeaks, it was possible to estimate the values of several coupling constants as listed in Table I. An estimate of the $^{13}C1$–$^{1}H1$ dipolar interaction was obtained from a magnitude ^{13}C–^{13}C COSY spectrum which was acquired with decoupling only during $t1$ (data not shown). The coupling constants are nearly within experimental error of the values observed for BDOG in 1:3 CHAPSO:DMPC, when normalized to account for the effects of $S_{micelle}$ in the liquid crystal. Given the sensitivity of splittings to headgroup orientation, it is highly probable that the headgroup of BDOG displays a structure in pure DMPC similar to that in 1:3 CHAPSO:DMPC mixtures.

B. Dependence on CHAPSO Concentration. A test for direct effects of CHAPSO with better spectral resolution can be achieved with *oriented* systems containing lower than usual amounts of CHAPSO or employing a detergent other than CHAPSO. Perturbations of structure which could be caused directly by CHAPSO would be expected to be dependent upon the CHAPSO:DMPC ratio. Therefore, the ^{13}C NMR spectrum of BDOG solubilized in a 1:4.85 CHAPSO:DMPC sample was acquired by both 1-D (Figure 2) and 2-D (DQF COSY, not shown) methods. A number of coupling constants were measured from these spectra and are listed in Table I. The corrected splittings for the 1:4.85 sample and 1:3 data generally show reasonable agreement.

It was recently observed that DMPC bilayers can be oriented by a magnetic field in the presence of the detergent Triton X-100.[40] A 1:3 Triton:DMPC sample containing a small amount of added [$^{13}C_6$]BDOG was prepared, and both normal (Figure 2) and double quantum filtered (INADEQUATE) 1-D spectra were taken. Coupling constants which were measured are listed in Table I. The "corrected splittings" are again in reasonable agreement with those from the 1:3 CHAPSO:DMPC sample. These results indicate that the observed headgroup structure of BDOG is largely independent of the presence of either Triton or CHAPSO.

C. Dependence on BDOG Concentration. BDOG is certainly associated with the CHAPSO–DMPC assemblies and is certainly influenced by the presence of a bilayer surface. However, it is still possible that BDOG may aggregate within the bilayer particles to form its own phase where glycoside–glycoside contacts may contribute to the observed conformation. This behavior has been observed previously for some native glycolipids and is generally

(48) Bax, A.; Kempell, S. P.; Freeman, R. J. *J. Magn. Reson.* **1980**, *41*, 349–353.
(49) Prestegard, J. H. Unpublished simulations.

Table II. Dipolar Coupling Constants Measured for the Alkyl Glycosides in 1:3 CHAPSO:DMPC at 40 °C[a]

	β-gal		β-2-deoxy		β-6-deoxy		α-glu		α-2-deoxy	
vector	obsd	cor	obsd	cor	obsd	cor	obsd	cor	obsd	cor
C1–C2	282 ± 20	240	|35 ± 40|	−75 or −5	|535 ± 20|	495	378 ± 20	336	126 ± 15	86
C1–C3			|140 ± 45|	140	0 ± 75	0			0 ± 50	0
C1–C5					0 ± 75	0			0 ± 50	0
C1–H1	|1230 ± 200|	−1400	|1940 ± 300|	−2110	|3010 ± 400|	−3180	|2220 ± 400|	−2370	−1880 ± 250	−2050
C2–C3			|400 ± 70|	360	0 ± 100	0	|180 ± 20|	−220	|85 ± 30|	−125
C3–C4	−270 ± 25.0	−228								
C4–C5	325 ± 20	285					380 ± 20	340	|100 ± 40|	60
C4–C6	|10 ± 30|	|10|	|65 ± 25|	−65	0 ± 75	0	0 ± 30	0	0 ± 50	0
C4–H1	|0 ± 600|	200							|2200 ± 400|	2370
C5–C6	−180 ± 15	−222	|165 ± 40|	−205	0 ± 100	0	−232 ± 20	−274	−165 ± 40	−205

[a] Corrected values have been adjusted to eliminate the effects of scalar coupling, +40 Hz for one bond ^{13}C–^{13}C coupling and +170 Hz for one bond ^{1}H–^{1}C coupling.

explained in terms of the propensity of glycolipid headgroups to participate in intermolecular hydrogen bonding at the interface.[15]

We have performed two experiments which may clarify this issue. First, labeled β-hexyl glucoside was synthesized and solubilized in the oriented lipid bilayers, and dipolar coupling constants were measured (Table I) by single (Figure 2) and 2-D DQF COSY (not shown) methods. The alkyl chain of β-hexyl glucoside is shorter by six carbons than that of BDOG and, at low concentrations, should not readily form even small aggregates within a bilayer because of the stress this would likely place upon the structural integrity of the bilayer. When this hexyl glucoside data is corrected for $S_{micelle}$ the normalized splittings are found to be in agreement with those from BDOG except that the splittings from hexyl glucoside are scaled down by a constant factor (ca. 0.58). This scaling stems from additional motional freedom possessed by the headgroup at the interface relative to BDOG and/or a higher fraction of the glucoside existing freely, but transiently, in isotropic solution. In either case the average orientation of BDOG and β-hexyl glucoside appear to be the same. This argues in favor of a lateral dispersion of the glucoside across the bilayer surface.

A related experiment involves checking for the BDOG concentration dependence of the structure. Even with BDOG dispersed laterally throughout the bilayers, it is possible that its concentration may be high enough so that the averaged structure is influenced by interactions between proximal BDOG. We titrated a 1:3 CHAPSO:DMPC sample with deuterated BDOG to raise the DMPC:BDOG mole ratio from 12:1 to 2.1:1 while maintaining a constant weight/volume total amphiphile concentration and monitoring the quadrupolar splittings of the 3,4,6-ring-deuterated glucopyranoside (data not shown). It was observed that the relative splittings changed little during the titration. Only a small and gradual scaling of all splittings by a final factor of 1.2 was observed. This suggests only small changes in $S_{micelle}$ or S_z at high levels of BDOG and no significant change in the average structure of the headgroup. These results further support the notion that the observed average structure is governed almost exclusively by BDOG–DMPC interfacial interactions.

Coupling Constants for the Alkyl Glycosides. As in the previous study of BDOG, most carbon–carbon couplings were measured from a combination of 1- and 2-D experiments employing samples with a high level of uniform ^{13}C labeling: 100% labeling for the headgroups of α-dodecyl glucoside and β- and α-tetradecyl 2-deoxyglucosides and 66% labeling for β-dodecyl 6-deoxyglucoside. In the previous work, determination of the magnitudes of the coupling constants proceeded smoothly because of the absence of strong coupling effects or complex multiplet patterns. This turned out to be a fortuitous consequence of the dispersion of the chemical shifts of the carbons and the sizes of the coupling constants exhibited by BDOG. In each case presented here, the ^{1}H decoupled, ^{13}C–^{13}C DQF COSY spectra (Figure 3) exhibited evidence of strong coupling between some spins. In some cases this completely prohibited assignment and measurement of coupling constants (see Figure 3B) while in other cases it resulted in an increase in the uncertainty of the value of the coupling constant. As an example of the problems encountered, consider the spectrum from the β-2-deoxyglucoside (Figure 3A). The crosspeak between C2 and C3 appears to represent the correlation of a simple pair of doublets. However, the coupling constant is different (405 vs 330 Hz) when measured along $f2$ as opposed to $f1$. This difference could arise from strong coupling or from differences in cancellation of antiphase components when small additional passive splittings exist in the direction of measurement. In cases where crosspeak asymmetry was observed, the coupling constants were assigned the average of the two extremes and the experimental uncertainty was increased to reflect this range.

In order to get around complications from strong coupling and complex multiplets, we synthesized β-dodecyl galactoside, α-dodecyl, 2,3-dideoxyhex-2-enoside, and α-dodecyl 2,3-dideoxyhexoside with uniform carbon labeling of only 15–20%. Unfortunately, we found that at the concentrations of the glycosides used in our samples, we were usually limited by sensitivity to one-dimensional spectroscopy: coupling constants can often be measured, but assignments are difficult. An INADEQUATE series run on the β-galactoside (see example in Figure 4) permitted the couplings between a number of directly bound carbons to be measured but did not allow unambiguous assignments of long range interactions, such as that clearly displayed as passive coupling at C1.

$^{13}C1$–$^{1}H1$ couplings were usually measured directly from the 1-D nondecoupled ^{13}C NMR spectrum of each glycoside. In all cases these appeared as simple doublets with no indication of the more complex multiplets expected to arise in the presence of strong coupling between H1 and proximal protons.[50] This is not surprising given the possible range of the ^{1}H–^{1}H coupling constants between vicinal protons in these samples and the relatively large shift difference between H1 and neighboring protons in these glycosides. Measurement of other ^{13}C–^{1}H coupling constants was in some cases accomplished by running ^{13}C–^{13}C COSY experiments with the decoupler on only during $t1$ (see example in ref 16).

In a number of cases involving C–H and C–C coupling, no splittings could be resolved and upper limits to the coupling constant were estimated based on the resonance line widths. The magnitudes of the coupling constants measured for the various glycosides are reported in Table II.

Properties of the α-2,3-Dideoxyglycosides. The alkyl glycosides for which data are reported in Tables I and II appear to be passive participants in a bilayerlike phase dominated by the properties of DMPC. This is supported by the fact that in each case the ^{13}C natural abundance peaks arising from the oriented lipid matrix exhibit essentially the same shifts as those seen in glycoside free preparations (data not shown). Also, samples containing each of those glycolipid analogs exhibited a phase transition from isotropic to oriented L_α-like phases as the temperature is raised through room temperature, an observation that appears to correlate with the gel to L_α transition for pure DMPC multibilayers at 24 °C.[1]

(50) French, A., Brady, R. O., Eds. *Computer Modeling of Carbohydrates*; ACS Symposium Series 430; American Chemical Society: Washington, DC, 1990.

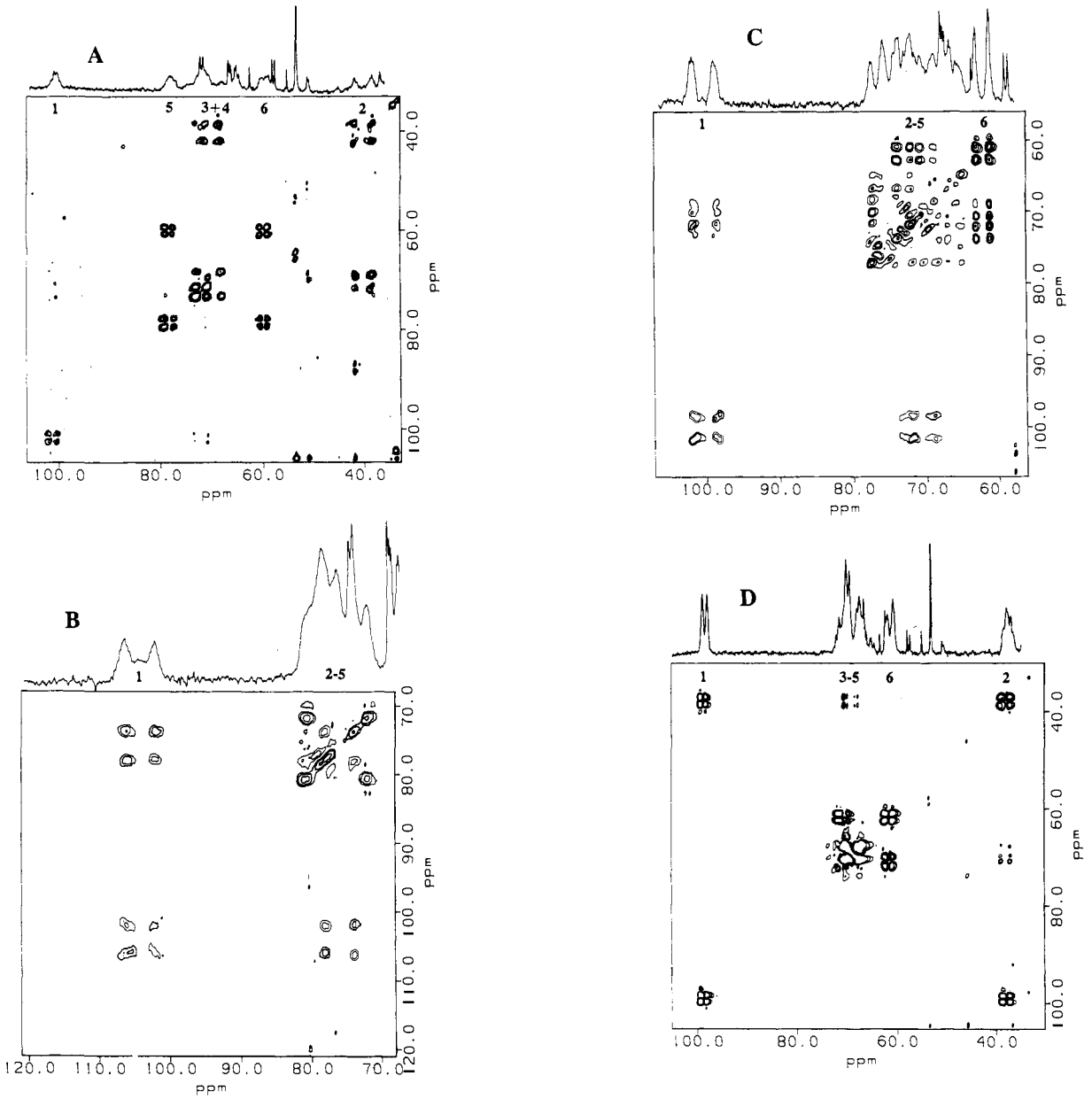

Figure 3. Double quantum filtered ^{13}C–^{13}C COSY spectra from the bilayer-associated alkyl glycosides at 40 °C. (A) β-Tetradecyl [$^{13}C_6$]-2-deoxyglucopyranoside (glycoside:DMPC = 1:19); (B) β-Dodecyl [$^{13}C_6$]-6-deoxyglucopyranoside (glycoside:DMPC = 1:17); (C) α-Dodecyl [$^{13}C_6$]glucoside (glucoside:DMPC = 1:14); (D) α-Tetradecyl [$^{13}C_6$]-2-deoxyglucopyranoside (glycoside:DMPC = 1:11). In each case the CHAPSO:DMPC ratio was 1:3, and the total lipid was 30% in 0.1 M KCl in D_2O. The spectral windows were the same in both dimensions in each case, and spectra were produced following exponential multiplication in $t2$ and both skewed sine and exponential multiplication in $t1$. Other parameters were as follows: (A) 128 $t1$ points representing 432 scans and 1024 data points each; spectral width = 9269 Hz; (B) 64 $t1$ points representing 1024 scans and 1024 data points each; spectral width = 6667 Hz; (C) 91 $t1$ points representing 592 scans and 1024 data points each; spectral width = 6410 Hz; (D) 128 $t1$ points representing 288 scans and 2048 data points each; spectral width = 9430 Hz. In the case of B, it should be noted that the lack of an observable C5–C6 correlation was due to the small size of the accompanying coupling constant. The sample temperature for B was 42.5 °C. Only the sugar carbon region of the 1-D spectra is shown.

The α-dodecyl 2,3-dideoxyglycosides appear to be an exception. Samples were prepared containing both α-dodecyl 2,3-dideoxy-hex-2-enopyranoside and α-dodecyl 2,3-dideoxyglucopyranoside in which the DMPC:glycoside ratio was 5:1 and the level of headgroup labeling was 15–20%. The ^{13}C NMR spectra of these samples show an unusual doubling of many peaks arising both from the DMPC matrix and the solubilized glycoside, suggestive of the formation of multiple phases; for example, the anomeric carbon near 100 ppm and the phosphocholine methyl near 58 ppm (Figure 5). The existence of two phases was supported by the ^{31}P NMR spectra of these samples (Figure 6) which shows (despite the breadth of the resonances due to the lack of ^1H decoupling) at least two distinct ^{31}P resonances arising from the DMPC phosphate. From the tendency of one member of each pair of ^{13}C resonances to be sharper and from the position of the most downfield ^{31}P peak, it is likely that one of these phases is isotropic. "Dilution" of the 2,3-dideoxyglycosides with DMPC to bring the glycoside:DMPC ratio to about 1:8 resulted in a significant reduction in the sharp component of the ^{13}C pairs relative to the broader components, suggesting that the putative isotropic phase forms as the result of a concentration-dependent breakdown of the bilayerlike phase by the dideoxy amphiphiles. It is most likely that the drastic increase in hydrophobic character of the glycosidic headgroups increases the ability of the sterically bulky rings to penetrate into the apolar region of the interface, making a more nearly spherical micelle the favored structure.

Signs of the Coupling Constants for the Alkyl Glycosides. Previously, we determined the signs of a number of coupling constants for BDOG by titrating the oriented sample with CHAPSO to scale down $S_{micelle}$ from its original value of −0.25

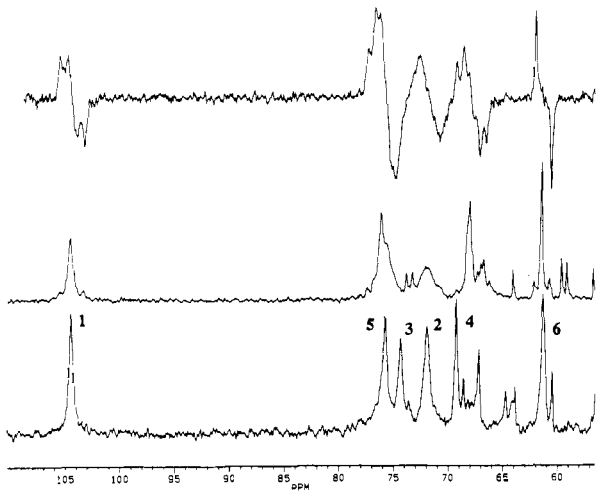

Figure 4. Carbon-13 (^{1}H-decoupled) NMR spectra of β-dodecyl [$^{13}C_6$]galactopyranoside (20% $^{13}C_6$) in 1:3 CHAPSO:DMPC, 30% total lipid in 0.1 M KCl in D_2O (glycoside:DMPC ratio = 1:5.4). Bottom, 53 °C (isotropic); middle, 40 °C (oriented); top, 40 °C INADEQUATE spectrum taken with the variable delay optimized for correlations of 220 Hz. Only the sugar carbon region of these spectra is shown.

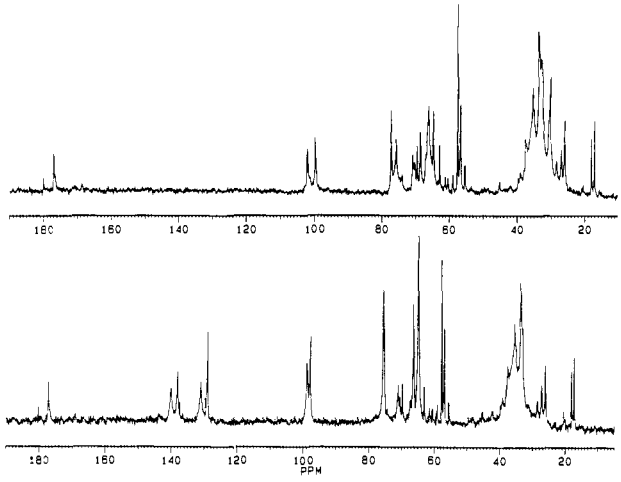

Figure 5. Carbon-13 (^{1}H-decoupled) NMR spectra of the 2,3-dideoxyglucosides in the usual DMPC:CHAPSO mixture at 40 °C. Bottom: α-dodecyl [$^{13}C_6$]-2,3-dideoxy-*erythro*-hex-2-enopyranoside (15–20% $^{13}C_6$):DMPC = 1:5); Top: α-dodecyl [$^{13}C_6$]-2,3-dideoxyglucopyranoside (15–20% $^{13}C_6$):DMPC = 1:5).

to its limit of 0.0 and taking advantage of the order independence of the (positive) scalar couplings. We used eq 11 to interpret our observed couplings:

$$\text{observed coupling} = S_{\text{micelle}} D_{i,j,\text{intrinsic}} + J \qquad (11)$$

where the intrinsic dipolar coupling refers to the non-S_{micelle} terms of eq 1. We should note that this equation also assumes that anisotropic parts of through-bond couplings will be small compared to the anisotropic parts of thorough-space dipolar couplings. This should be true where Fermi contact mechanisms dominate through-bond coupling. According to eq 11, observed splitting will pass either through 0 on its way to J (if $D_{i,j}$ is negative) or will converge directly to 0.0. This method presumes that the average structure of a headgroup is independent of the CHAPSO:DMPC ratio.

In this work a somewhat different method was adopted for scaling down the dipolar couplings without varying the CHAPSO:DMPC ratio. The method involves lowering the total amphiphile content to 20% (w/v) and then lowering the temperature from 40 to about 20 °C. We have found (for 1:3 CHAPSO:DMPC samples) that as the temperature approaches room temperature, the splittings are reduced and eventually converge to their isotropic limits around 22 °C. This phenomenon is only

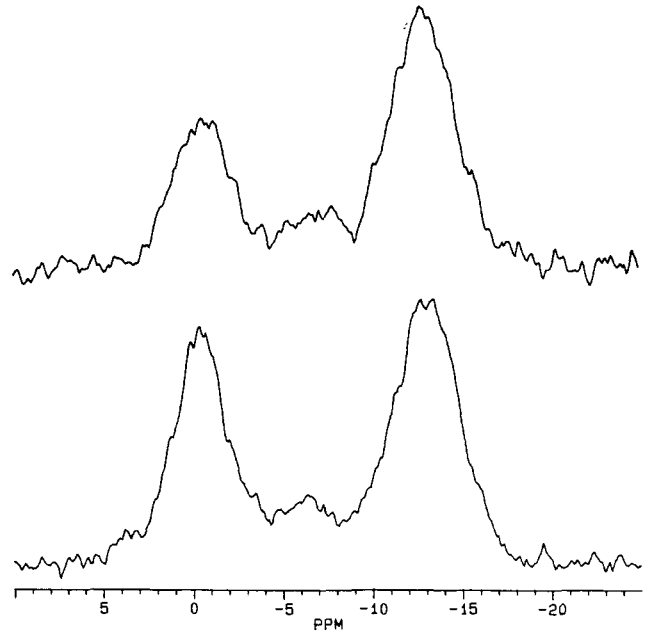

Figure 6. Phosphorus-31 (proton coupled) NMR spectra of the 2,3-dideoxyglucoside samples described in Figure 5 at 40 °C. Spectra are referenced to external phosphoric acid. Top: α-dodecyl [$^{13}C_6$]-2,3-dideoxy-*erythro*-hex-2-enopyranoside (15–20% $^{13}C_6$); Bottom: α-dodecyl [$^{13}C_6$]-2,3-dideoxyglucopyranoside (15–20% $^{13}C_6$).

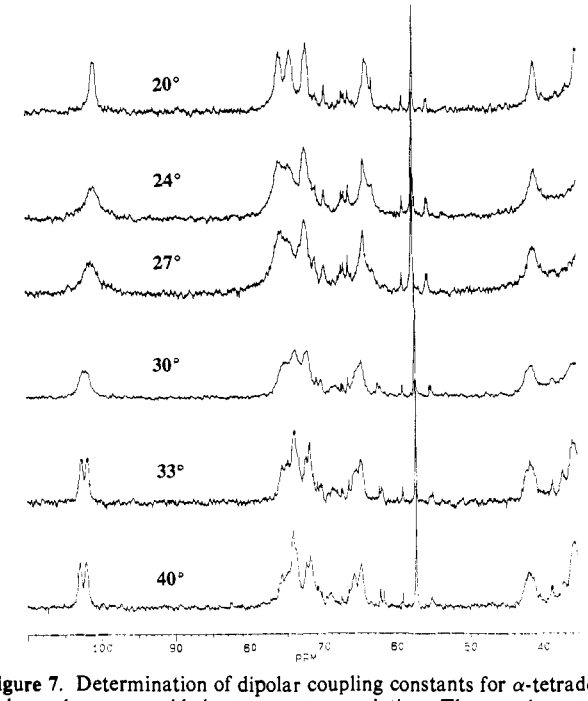

Figure 7. Determination of dipolar coupling constants for α-tetradecyl 2-deoxyglucopyranoside by temperature variation. The sample containing the 2-deoxyglucoside described in Figure 3 was diluted to 20% total lipid by adding D_2O prior to acquisition of this series of spectra. Only the sugar carbon region of the carbon-13 (^{1}H-decoupled) NMR spectra is shown.

observed in CHAPSO-rich mixtures and appears to be related to the gel to liquid crystalline phase transition of hydrated DMPC which occurs near 24 °C. In the cases of α-dodecyl glucoside and α-tetradecyl 2-deoxyglucoside some signs were successfully assigned (Table II). Figure 7 shows the data for the α-2-deoxyglycoside. The C1–C2 splitting at C1 (103 ppm) converges directly to its final value while the C5–C6 splitting at C6 (66 ppm) passes through zero, suggesting that the C1–C2 dipolar coupling is positive while the C5–C6 coupling is negative. In the case of β-dodecyl galactoside the original CHAPSO titration method was used to scale down S_{micelle} and determine signs (Table II). In other

Table III. Results from ORDERTEN Calculation of the Headgroup Orientation and Dynamics of the Bilayer-Associated Alkyl Glycosides from Dipolar Coupling Data

	BDOG	β-gal	β-2-deoxy	β-6-deoxy	α-glu	α-2-deoxy
increment of order parameters used in initial matrix search to find data sign combinations	0.02	0.05	0.05	0.05	0.05	0.05
no. of satisfactorily signed sets of data	1	1	3	2	2	1
increment used in order matrix search using the individual sets of signed data	0.02	0.03	0.05	0.05	0.05	0.05
no. of distinctly signed sets of solutions	1	1	2	1	1	1
final incrementation of the order matrix using the final data set (see Table II)	0.016	0.03	0.05	0.04	0.045	0.025
no. of signed data sets which lead to satisfactory solutions	1	1	2	1	1	1
no. of final satisfactory solutions	52	17	47	48	12	23
increment used with signed and unsigned data sets to verify above solutions using rms cutoff	0.03	0.0375	0.0375	0.0375	0.0375	0.0375
acceptable ranges of parameters within the solution sets						
S_z	0.31–0.38	0.28–0.46	0.45–0.65	0.42–0.54	0.38–0.54	0.37–0.57
η	0.15–0.53	0.03–0.95	0.16–0.85	0.39–0.98	0.17–0.87	0.15–0.92
β	27–36	27–49	6–35	47–80	49–70	42–58
γ	74–89	58–90	54–138[a]	63–79	40–55	17–27
α	−28 to −57	−33–90	−86–28[a]	71–108	9–100	42–115
axial symmetry assumption results[b]						
incrementation of Euler angles β and γ	1°	1°	1°	0.67°	0.67°	0.67°
incrementation of S_z-axial	0.02	0.02	0.01	0.01	0.01	0.01
no. of satisfactory solutions	5	15	1	1	12	1
range of acceptable S_z	0.40–0.42	0.38–0.46	0.97 (least sq fit)	0.52 (least sq fit)	0.50–0.56	0.42 (least sq fit)
range of acceptable β	28–30	26–30	15	61	48–54	44
range of acceptable α	66–68	−61 to −73	26	80	37–43	17

[a] Solutions with $\beta < 10$ were excluded from the calculation of γ and α ranges. [b] In ORDERTEN, under axial symmetry assumption conditions, the program directly increments Euler angles (see eq 6 and 7) rather than order parameters.

cases, we were not able to determine signs because of excessive broadening near the isotropic transition or because of difficulties in sample preparation.

Determination of the Averaged Interfacial Headgroup Structures for the Alkyl Glycosides. A. Order Matrix Results. We pursued an iterative strategy for locating the ranges of orientations and order parameters in agreement with experimental data for each glycoside (see Materials and Methods). First, the "uncorrected" data sets from Table II were used to find solutions which fit all of the data within experimental error. For those measurements of unknown sign and for which J is significant, the uncertainty was set to the sum of the experimental error and J. In each case this calculation led to one or more *families* of solutions for which the predicted signs were uniform *within* each family (see Table III). For example, it was found that the uncorrected β-dodecyl 6-deoxyglucoside data could be satisfied by sets for which C1–C2 and C1–H1 were either +/− or −/+, respectively. Based on these predicted signs, the coupling constants were corrected for scalar coupling and the error reduced by J so that each "family" of preliminary solutions led to one new data set.

Each *corrected* data set was input, and the matrices were again searched as the second step of the iterative process. With the exception of the β-2-deoxyglucoside, only one of the possible corrected data sets led to acceptable solutions (see Table III). In the case of the exception, two of the data sets, differing only in the sign of the small C1–C2 dipolar coupling (see Table II), led to acceptable solutions. However, it was observed that these solutions represented very similar orientations of the β-2-deoxy headgroup. Thus, for each alkyl glycoside, only a single family of related solutions was obtained.

As a final check on our results, the order matrix calculation was run on both the "uncorrected" and final data sets of Table II using the weighted mean variation between the experimental and predicted data sets as the criterion for saving or discarding order matrix solutions. In this manner, a check was made for the existence of solutions which satisfied most of the data, but for which one or possibly two data points had problems. We did not find any solutions which were not clearly related to the final solution sets determined in the second stage above, indicating that the solutions described in Table III represent the only satisfactory fits of the data.

The structural parameters listed in Table III can be thought of in the following manner. The orientation of the molecule with respect to the bilayer normal is defined exclusively by Euler angles β and γ while the motional order of the director is defined by S_z. The location of the x and y principal order axes within the molecular frame also requires definition of Euler angle α. The asymmetry of motion about the principle order axes x and y is given by η which is equal to $(S_x - S_y)/S_z$. The orientations of the glycosides were well-defined by the data. In the case of each glycoside, except for β-tetradecyl 2-deoxyglucopyranoside, a rather narrow range of β and γ is displayed, indicating that the headgroup orientation of the glucoside with respect to the bilayer normal is well-defined. In the case of the β-2-deoxyglucoside the large range for γ is more a result of β being near to 0, than imprecision in structure determination. (When $\beta = 0$, orientation is effectively independent of γ).

α is best defined in the cases of BDOG, β-dodecyl 6-deoxyglucoside, and α-tetradecyl 2-deoxyglucoside, making the placement of the x and y order axes within the molecular frame most definitive for these glycosides. The β-2-deoxyglucoside shows a much larger range of α values but, as in the case of γ, this is partly the result of a small β value. Eliminating solutions with smaller β values or restricting consideration to only ones coming from choosing the C1–C2 coupling as negative restricts the α range to limits similar to those for BDOG.

S_z values are moderately well-determined in all cases and should provide a useful basis for comparison of molecular properties. Only in the cases where α is well-defined is η, the asymmetry parameter, meaningful. η varies significantly in the four cases mentioned above, but should nevertheless allow some useful comparison.

B. Axial Symmetry Assumption. Iterative calculations were also run in a manner similar to that for the full order matrix except that motion was assumed to be axially symmetric about the bilayer normal. For α-dodecyl glucoside, β-dodecyl galactoside, and BDOG the final corrected data sets led in each case to a single family of closely related structures. In the case of β-tetradecyl 2-deoxyglucoside, α-tetradecyl 2-deoxyglucose, and β-dodecyl 6-deoxyglucoside no solutions were found which satisfied *all* of the data within experimental error. In the last two cases, eqs 6 and 7 were utilized with a least squares fitting program (MINSQ, Micromath Software, Salt Lake City, UT) to determine the best

Table IV. Observed and Predicted σ_{an} for Alkyl Glycosides in 1:3 CHAPSO at 40 °C[a,b,c]

	BDOG	β-gal	β-2-deoxy	α-glu	α-2-deoxy
C1[d]					
observed	−0.2	−1.13	1.7	0.80	1.60
predicted (1)				0.23–1.06	0.64–1.51
predicted (2)				−0.06 to 0.93	0.09–0.87
$(\sigma_1 - \sigma_2)_{max}$				0.31	0.9
C2					
observed	−0.1	−0.50			
predicted (1)	−0.36 to −0.76	−0.12 to −1.0			
predicted (2)	−0.31 to −0.52	0.06 to −0.69			
$(\sigma_1 - \sigma_2)_{max}$	0.32	0.55			
C3					
observed	1.20	1.20			
predicted (1)	0.0–0.73	−0.41 to 1.32			
predicted (2)	0.43–1.22	0.01–1.75			
$(\sigma_1 - \sigma_2)_{max}$	0.51	0.51			
C4					
observed	0.25	−1.1			0.0
predicted (1)	0.99–1.11				0.21–1.49
predicted (2)	0.66–0.78				0.19–1.52
$(\sigma_1 - \sigma_2)_{max}$	0.39				0.62
C5					
observed	1.00	0.40	2.4		−1.5
predicted (1)	0.38–0.53	0.06–0.44	2.03–2.80		−0.87 to −1.20
predicted (2)	1.28–1.44	0.95–1.23	1.17–1.87		−1.38 to −1.70
$(\sigma_1 - \sigma_2)_{max}$	0.93	0.96	1.04		0.36
C6[e]					
observed	−0.75	0.15	−1.3		1.5

[a] (1) and (2) correspond to the α-methyl and α-phospho glucoside tensor sets, respectively. [b] $(\sigma_1 - \sigma_2)_{max}$ is the maximum observed difference in predicted σ_{an} for the two models for any one order matrix solution in the entire set of solutions. [c] The errors associated with each observed σ_{an} are on the order of 0.2 ppm. [d] CSA values were not predicted for the β-anomeric carbons or the galactose C4 because of the unsuitability of the α-anomeric carbons and the glucosyl C4 carbon as models for these. [e] CSA values for C6 were not predicted because of a lack of information regarding the torsion angle associated with C5–C6.

fit of the data. In the case of β-tetradecyl 2-deoxyglucoside, a manual search for the solution with the best root mean square deviation value was executed. The results from ORDERTEN and from the least squares fitting are listed in Table III. For each glycoside the possible orientations obtained when axial symmetry is assumed are very similar to the range of structures obtained when no such assumption is made. It appears that even in cases when anisotropy is measurable, assumption of axial symmetry gives a reasonable preferred orientation for the headgroup. It, of course, precludes any interpretation of anisotropies of motion which may, in fact, be present, and such asymmetry may well be the source of failure to find structures for α-2-deoxyglucose, β-2-deoxyglucose, and β-6-deoxyglucose using normal error limits. The ability to make an axial symmetry assumption with some confidence is, nevertheless, important because it reduces the number of variables needed to define the orientation from 5 to 3. This is clearly an advantage when data are scarce.

^{13}C Chemical Shift Anisotropy Data. As presented in the Theory and Calculations section, chemical shift anisotropy can provide data on order tensor elements in much the same way as dipolar coupling data. ^{13}C shift tensors have been determined for carbons in α-phospho glucopyranoside and α-methyl glucopyranoside,[26,27] providing suitable models for most carbons in the sugars studied here. Because the anisotropies of these shift tensors are rather small, however, we chose not to include them directly in our search for order tensor elements, but utilized them as an after-the-fact check on the accuracy of our solutions.

Where resolution and the absence of strong ^{13}C–^{13}C coupling effects allowed, the anisotropies of the chemical shifts for the labeled glycosyl carbons were measured simply by subtracting the isotropic chemical shift from the oriented sample chemical shift. The isotropic shifts were obtained from the CHAPSO–DMPC samples in which the oriented to isotropic transition had been induced by CHAPSO addition or dilution/temperature variation as described previously. A straightforward example is given for β-dodecyl galactoside in Figure 4, where the resonances in the oriented spectrum show substantial shifts relative to those in the same sample which had been made isotropic. These chemical shifts are listed in Table IV. The ranges of σ_{an} predicted for order matrix solutions of Table III are listed in Table IV. This table also lists the maximum deviation between observed values and values predicted based on the methyl glycoside and the phospho glucoside tensor data. The latter, along with an estimated uncertainty of ±0.3 ppm for experimental data, provide an indication of the possible significance of the comparisons.

Several observations can be made. First, the observed chemical shifts generally correlate with the predicted chemical shifts. This tends to support the validity of our order matrix methodology and the orientations determined. However, the variations in the predicted σ_{an} for each set are large, prohibiting a more quantitative structural analysis. This problem stems as much from variation in the CSA tensors of the model compounds as it does from experimental data and suggests that the carbon-13 tensors of the carbons of simple carbohydrate monomers are quite dependent upon the detailed covalent bonding and stereochemistry of the structure. One additional point of interest is the magnitudes of σ_{an} observed for the various C6s. These are, in most cases, as large as those observed for the endocyclic carbons. We did not predict shifts for these carbons because of uncertainty about the C4–C5–C6–O6 dihedral angle, but the magnitudes suggest that little additional averaging of the C6 tensor by internal bond rotation about C5–C6 occurs for the interfacial alkyl glycosides.

To summarize, some useful information from CSA effects have been obtained. However, the relatively small $\Delta\sigma$ for hydroxylated hydrocarbons and the apparent tensor dependence upon small functional differences among sites appears restrictive. CSA information has, of course, been useful in analysis of other types of amphiphilic molecules[22-25] and may be useful for carbohydrates containing carbonyl moieties that have large and well-defined CSA values.

Discussion

The headgroup orientations of the interfacial alkyl glycosides are illustrated in Figure 8. The structures shown are representative solutions from the order matrix search for each glycoside which has Euler angles near the mean values for each set. The conformations of the 6-hydroxymethyl groups were not determined, but the groups were rotated after determining the orientation so

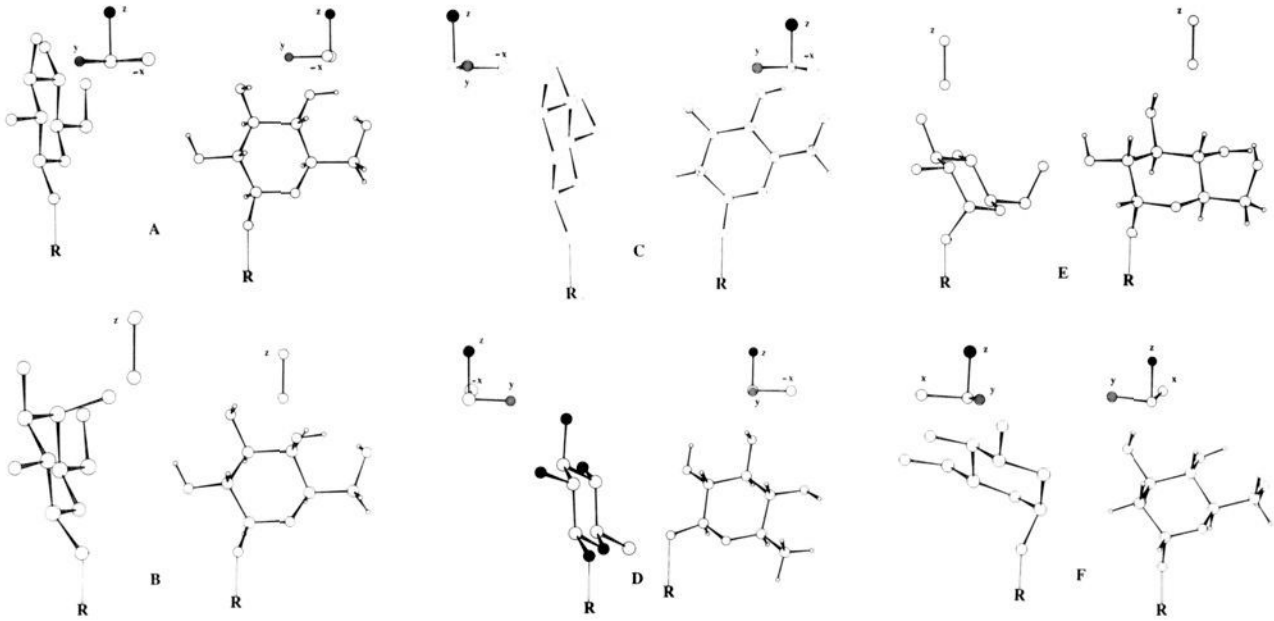

Figure 8. Interfacial orientations of the alkyl glycoside headgroups in DMPC–CHAPSO bilayers. (A) β-Dodecyl glucopyranoside; (B) β-dodecyl galactopyranoside (C) β-tetradecyl 2-deoxyglucopyranoside; (D) β-dodecyl 6-deoxyglucopyranoside; (E) α-dodecyl glucopyranoside; (F) α-tetradecyl 2-deoxyglucopyranoside. In the cases of B and E the location of the x and y order axes are not depicted because of uncertainty in α. Side views of the structures are shown without hydrogens for the sake of clarity. R in each case represents the alkyl chain. The pseudobonds drawn to R as well as the z order axes illustrate the direction of the bilayer normal.

that the hydroxy group faces away from the interface. The structures determined under the axial symmetry assumption are not shown, but are pictorially similar to the depicted solutions.

The structures of the β-glycosides provide the most insight into our previous observations regarding BDOG (Figure 8A). Removal of the 6-hydroxyl clearly results in the tipping of the glucose ring around the ring normal so that the 6-methyl reorients towards the apolar region of the interface (Figure 8D). This is consistent with an optimization of hydrophobic interactions between the methyl group and apolar lipid moieties. Removal of the 2-OH causes the ring to tip slightly in the opposite direction optimizing contact between the 2-methylene and the hydrophobic region (Figure 8C). β-Dodecyl galactoside (Figure 8B) is observed to have the same headgroup orientation as BDOG, suggesting that the 4-position clears the polar–hydrophobic interface and plays little role in defining the energetics of the headgroup–interface interaction. These results are clearly consistent with the model earlier proposed to account for the observed headgroup orientation of BDOG. The S_z order parameters of the β-2-deoxy compound and the β-6-deoxyglucoside are also larger than those of the galactoside and BDOG. While this could be due to other factors, it is consistent with increased hydrophobic interactions of the headgroups with the interface.

The structures of the two α-glycosides (Figure 8E and F) are markedly different from their corresponding β anomers. Nevertheless, they can be rationalized along lines similar to those used for BDOG. The α linkages require that the plane of the sugar ring become more nearly parallel to the plane of the bilayer if a simple extension of the alkyl chain along the bilayer normal is to be maintained. A preference for the alkyl chains to extend as straight as possible through the sterically constrained DMPC interfacial lattice, along with the known tendency of individual glycosides to favor certain glycosidic torsion angles,[8,51] probably combine to yield the observed orientation. The most energetically costly interaction produced by this initial preference is likely to involve the increased proximity of the 2-OH to the interface. The structure of the α-dodecyl glucoside appears to compensate for this effect because its ring has also rotated along an axis approximately coinciding with C1–C4 to increase the distance of the 2-hydroxyl from the interface at the expense of bringing the more hydrophobic 6-methoxyl closer. This rotation is not required (or observed) in the case of the α-2-deoxy compound because of the absence of a polar group at C2.

It is noteworthy that in most cases the more hydrophobic compounds also tend to have better defined x and y axis orientations (α range) and a somewhat higher range of asymmetry parameters. Interpretation of asymmetry parameters is not always straightforward since they may be the result of restrictions imposed by both the local energetics of rotation about glycosidic bonds and the presence of a membrane interface. Moreover, there is never a unique mapping between an asymmetry parameter and a model for motion. Previously, we had assumed a model having small oscillations about an average structure to suggest that the asymmetry seen for DBOG could be correlated with interaction between the 2-OH or 6-CH_2OH and the membrane interface. For the α-2-deoxy case and the β-2-deoxy case (Figure 8F and C) similar arguments seems to hold. Rotation about x would tend to vary interactions between the 2-deoxy or 6-hydroxy group and the membrane interface more than rotation about y. Hence, rotation about x is more restricted. Data for the β-6-deoxy molecule, the other example with a well-determined axis location and asymmetry parameter, seems to contradict this simple interpretation. It may well be that restricted motion about the C_1–O_1 glycosidic bond is the dominant effect in the β-6-deoxy molecule, or it may be that motion is more complex than simple oscillation about an averaged structure.

While our experimental methods yield no direct evidence regarding the depth to which the glycosides extend into the DMPC interface, the data do suggest a rather general model for the placement of the headgroups of the alkyl glycosides at the DMPC interface. The phosphocholine headgroups (which possess both ions and a nonpolar ethylene moiety) are, on the average, thought to lie nearly in the bilayer plane[51,52] and probably form an average surface which is dominated by the polarity of the phosphodiester and quaternary ammonium ions, but which contains local hydrophobic patches. The fact that the orientation of BDOG is the same as that of the corresponding galactoside suggests that C4 is well beyond the surface. On the other hand, the sensitivity of the observed glycoside structures to changes at the 2 and 6

(51) Hauser, H.; Pascher, I.; Pearson, R. H.; Sundell, S. *Biochim. Biophys. Acta* **1981**, *650*, 21–51.

(52) Weiner, M.; White, S. *Biophys. J.* **1992**, *61*, 434–447.

positions suggests the C2–C1–O5–C6 part of these glycosides sits directly upon, or slightly into, the phosphocholine surface. One must, of course, remember that in both the case of DMPC and the case of the glycoside we are dealing with highly averaged structures.[52,53]

Thus, we have been able to build a generally coherent picture of the average conformation and orientation of a series of simple glycosides at a membrane interface. The series suggests the importance of some hydrophobic interactions at the membrane interface in addition to the more often cited hydrogen-bonding interactions. It would appear that extension of the specific developments reported herein to a wider class of molecules and to more biologically relevant structures would be possible. If so, it should be possible to build a sound physical basis for understanding the interactions of glycolipids with membrane components.

Acknowledgment. We thank Brian Hare and Kathleen Howard for their generous assistance in running computations and Yves Aubin for synthesizing β-dodecyl galactose. Dr. Yuying Gosser is acknowledged for her work on interpretation of chemical shift anisotropy effects. Support for this work was provided by the NIH Grant GM33225. C.R.S. was supported by NIH Fellowship GM 13227.

(53) DeLoof, H.; Harvey, S.; Segrest, J.; Pastor, R. *Biochemistry* **1991**, *30*, 2099–2113.

Structure of the Radical Cations of *N,N'*-Polymethylene-*syn*-1,6:8,13-diimino[14]annulenes: An ESR and ENDOR Study

Fabian Gerson,*,† Georg Gescheidt,† Jürgen Knöbel,†,§ William B. Martin, Jr.,†,⊥ Ludger Neumann,‡ and Emanuel Vogel‡

Contribution from the Institut für Physikalische Chemie der Universität Basel, Klingelbergstrasse 80, CH-4056 Basel, Switzerland, and Institut für Organische Chemie der Universität Köln, Greinstrasse 4, D-5000 Köln 41, FRG. *Received March 6, 1992*

Abstract: *N,N'*-Polymethylene-*syn*-1,6:8,13-diimino[14]annulenes, **1–7**, in which the number, *m*, of CH_2 groups varies from 1 to 7, and *N,N'*-dimethyl-*syn*-1,6:8,13-diimino[14]annulene (**8**) were synthesized. The radical cations of **1–8**, as well as those of several derivatives of **1–4**, have been studied by ESR, ENDOR, and TRIPLE resonance spectroscopy. In contrast to the corresponding anions $\mathbf{1}^{\bullet-}$–$\mathbf{8}^{\bullet-}$, which are bridged π-perimeter radicals, the cations $\mathbf{1}^{\bullet+}$–$\mathbf{8}^{\bullet+}$ must be considered as N-centered radicals with the bulk of the spin population residing at the two heteroatoms. The structure and properties of these radical cations critically depend on the length of the polymethylene chain linking the N atoms. When the number, *m*, of the CH_2 groups in this chain is 1 or 2, the N lone pairs are directed "outward", so that their interaction is relatively weak. Thus, the radical cations $\mathbf{1}^{\bullet+}$ (m = 1) and $\mathbf{2}^{\bullet+}$ (m = 2) are thermodynamically and kinetically rather unstable, and their ^{14}N coupling constant, a_N, is only 0.6–0.7 mT. On the other hand, with m = 3–7 the N lone pairs point "inward", an arrangement that favors the formation of an N–N three-electron σ-bond. The pertinent radical cations $\mathbf{3}^{\bullet+}$–$\mathbf{7}^{\bullet+}$ (m = 3–7) exhibit unusual thermodynamic and kinetic stabilities which, in two cases ($\mathbf{3}^{\bullet+}$ and $\mathbf{4}^{\bullet+}$), allowed X-ray crystallographic structure analyses to be carried out. The coupling constant a_N amounts to 1.70 mT for $\mathbf{3}^{\bullet+}$, and it increases further to an almost constant value of 2.57–2.72 mT for $\mathbf{4}^{\bullet+}$–$\mathbf{7}^{\bullet+}$; an a_N value of 2.66 mT is also observed for $\mathbf{8}^{\bullet+}$, which may be regarded as having its N atoms linked by a very long polymethylene chain. The changes in the coupling constant a_N along the $\mathbf{1}^{\bullet+}$–$\mathbf{7}^{\bullet+}$ ($\mathbf{8}^{\bullet+}$) series can be rationalized in terms of the varying "s-character" of the singly occupied orbital centered at the spin-bearing N atoms.

Introduction

Derivatives of *syn*-1,6:8,13-diimino[14]annulene,[1,2] in which a polymethylene chain links the two N atoms, are ideal models for the studies of the interaction between such nonbonded but spatially close atoms. That is because the geometry and electronic structure of the N atoms in these derivatives can systematically be modified by varying the number of the CH_2 groups in the linking chain. The corresponding radical cations are particularly suitable for the studies in question, as ionization can lead to the formation of an N–N three-electron σ-bond[3–7] and as the unpaired spin is appropriate to probe the N–N interaction.[3b,4–6]

The present paper deals with ESR and ENDOR investigations on the radical cations of several *N,N'*-alkanediyl-*syn*-1,6:8,13-diimino[14]annulenes where alkanediyl is methylene (**1**), perdeuteriomethylene (**1**-d_2), isopropylidene (**1**-Me_2), perdeuterioisopropylidene (**1**-$(CD_3)_2$), dimethylene (**2**), perdeuteriodimethylene (**2**-d_4), trimethylene (**3**), 2,2-dideuteriotrimethylene (**3**-d_2), tetramethylene (**4**), 2,2,3,3-tetradeuteriotetramethylene

* Author to whom correspondence should be addressed.
† Universität Basel.
‡ Universität Köln.
§ Present address: F. Hoffmann-La Roche AG, CH-4058 Basel, Switzerland.
⊥ Professor Emeritus, Department of Chemistry, Union College, Schenectady, NY 12309.

(1) (a) Vogel, E.; Kuebart, F.; Marco, J. A.; Andrée, R.; Günther, H.; Aydin, R. *J. Am. Chem. Soc.* **1983**, *105*, 6982. (b) Destro, R.; Pilati, T.; Simonetta, M.; Vogel, E. *J. Am. Chem. Soc.* **1985**, *107*, 3185.

(2) (a) Vogel, E. *Lect. Heterocycl. Chem.* **1985**, *8*, 103. Andrée, R. Dissertation, Universität Köln, Germany, 1985. Becker, D. Diplomarbeit, Universität Köln, Germany, 1985. (b) Destro, R.; Pilati, T.; Simonetta, M.; Vogel, E. *J. Am. Chem. Soc.* **1985**, *107*, 3192. (c) Wolfrum, P. Dissertation, Universität Köln, Germany, 1990. (d) Houriet, R.; Feng, W.; Vogel, E.; Wolfrum, P.; Schwarz, H. *Int. J. Mass. Spectrom. Ion Processes* **1989**, *91*, R1.

(3) (a) Alder, R. W. *Acc. Chem. Res.* **1983**, *16*, 321 and references therein. (b) Kirste, B.; Alder, R. W.; Sessions, R. B.; Bock, M.; Kurreck, H.; Nelsen, S. F. *J. Am. Chem. Soc.* **1985**, *107*, 2635. (c) Alder, R. W.; Orpen, A. G.; White, J. M. *J. Chem. Soc., Chem. Commun.* **1985**, 949.

(4) Gerson, F.; Knöbel, J.; Buser, U.; Vogel, E.; Zehnder, M. *J. Am. Chem. Soc.* **1986**, *108*, 3781.

(5) Gerson, F.; Gescheidt, G.; Buser, U.; Vogel, E.; Lex, J.; Zehnder, M.; Riesen, A. *Angew. Chem., Int. Ed. Engl.* **1989**, *28*, 902.

(6) Dinnoncenzo, J. P.; Banach, T. E. *J. Am. Chem. Soc.* **1988**, *110*, 971.

(7) For theoretical work, see: Bouma, W. J.; Radom, L. *J. Am. Chem. Soc.* **1985**, *107*, 345. Gill, P. M. W.; Radom, L. *J. Am. Chem. Soc.* **1988**, *110*, 4931.

0002-7863/92/1514-7107$03.00/0